Electrochemical study of an electron shuttle diheme protein: The cytochrome c550 from T. thermophilus

Frédéric Mélin, Barbara Schoepp-Cothenet, Saleh Abdulkarim, Mohamed R. Noor, Tewfik Soulimane, Petra Hellwig

Electrochemical study of an electron shuttle diheme protein: The cytochrome c_{550} from *T. thermophilus*

Frederic Melin [a,*], Barbara Schoepp-Cothenet [b], Saleh Abdulkarim [c], Mohamed R. Noor [c,*], Tewfik Soulimane [c], Petra Hellwig [a]

[a] *Laboratoire de Bioélectrochimie et Spectroscopie, Chimie de la Matière Complexe, UMR 7140, Université de Strasbourg, CNRS, 4 Rue Blaise Pascal, 67000 Strasbourg, France*

[b] *Aix-Marseille Univ., CNRS, BIP UMR 7281, FR 3479, IMM, 13402 Marseille Cedex 20, France*

[c] *Chemical Sciences Department & Bernal Research Institute, University of Limerick, Limerick, Ireland*

*Corresponding authors: F. Melin (email: fmelin@unistra.fr, phone: +33 3 68 85 16 35), M. R. Noor (email: Mohamed.Noor@ul.ie)

ABSTRACT:

Cytochrome c_{550}, a diheme protein from the thermophilic bacterium *Thermus thermophilus*, is involved in an alternative respiration pathway allowing the detoxification of sulfite ions. It transfers the two electrons released from the oxidation of sulfite in a sulfite:cytochrome *c* oxidoreductase (SOR) enzyme to heme/copper oxidases via the monoheme cytochrome c_{552}. It consists of two conformationally independent and structurally different domains (the C- and N-terminal) connected by a flexible linker. Both domains harbor one heme moiety. We report here the redox properties of the full-length protein and the individual C- and N-terminal fragments. We show by UV/Vis and EPR potentiometric titrations that the two fragments exhibit very similar potentials, despite their different environments. In the full-length protein, however, the N-terminal heme is easier to reduce than the C-terminal one, due to cooperative interactions. This finding is consistent with the kinetic measurements which showed that the N-terminal domain only accepts electrons from the SOR. Cytochrome c_{552} is able to interact with its partners both through electrostatic and hydrophobic interactions as could be shown by measuring efficient electron transfer at gold electrodes modified with charged and hydrophobic groups, respectively. The coupling of electrochemistry with infrared spectroscopy allowed us to monitor the conformational changes induced by electron transfer to each heme separately and to both simultaneously.

KEYWORDS: multi heme proteins, bioelectrochemistry, potentiometric titration, EPR spectroscopy, FTIR spectroscopy, *Thermus thermophilus*.

1. Introduction

Biological energy conversion processes such as respiration and photosynthesis rely on efficient inter-and intra-protein electron transfer (ET) reactions [1-3]. In both the photosynthetic and respiratory chains, the transport of electrons between the enzymes embedded in the membrane is accomplished either by molecules freely diffusing in the membrane, the quinones, or water soluble electron carrying proteins, such as cytochrome (cyt) *c*. This small monoheme protein (12.5 kDa) [4-6], which transfers electrons between cyt bc_1 complex and cyt *c* oxidase in the mitochondrial respiratory chain, has long served as a model system for mechanistic studies of protein ET processes. Important insight into the distance dependence and reorganization energy of the ET process has been gained from protein film voltammetry studies of cyt *c* immobilized on electrodes modified with various functional groups including alkyl [7], pyridyl [8, 9], amino [10, 11], carboxyl [12-14], L-cysteinyl [15] and hydroxyl [16]. In particular, studies at metallic surfaces modified with ω-carboxyl alkanethiols by a combined approach of electrochemistry, surface-enhanced and time-resolved spectroscopic techniques have provided a full image of the electron transfer dynamics of electrostatically immobilized cyt *c* and have highlighted the important role of electric field effects in the ET properties [17-21]. These surfaces have been designed to mimic the interaction between cyt *c* and cyt *c* oxidase, which is believed to involve a cluster of positively charged lysines residues on cytochrome *c* and several carboxylate groups of aspartic and glutamic acid residues on the oxidase [22-24].

Homologous electron carrier proteins from bacterial respiration chains have been less extensively studied. They often exhibit significantly different structural features, like for example the cyt c_{552} from the thermophilic bacterium *Thermus thermophilus*, which possesses only uncharged residues around the exposed heme edge [25-27]. Mainly hydrophobic interactions are thus believed to take place between cyt c_{552} and the corresponding cyt *c* oxidases in *T. thermophilus* [25, 28, 29]. Bacteria also use diheme proteins to transfer electrons between the respiratory enzyme complexes, such as the cyt c_4, which are native electron donors of C family (cbb_3) oxidases [30, 31]. They are the simplest model systems for multi heme proteins [31-34]. Recently, a diheme electron carrier protein with 15% sequence identity only to cyt c_4 was identified from *T. thermophilus* [35]. It was called cyt c_{550}, on the basis of its spectral properties. It is involved in an alternative respiration pathway using sulfite ions instead of nicotinamide adenine dinucleotide as initial electron donor [35]. This pathway also allows the detoxification of the highly reactive sulfite ions. Cyt c_{550} receives electrons from the enzyme responsible for oxidation of sulfite, the sulfite:cytochrome *c* oxidoreductase (SOR), and further transfer them to the terminal cyt ba_3 and caa_3 oxidases through cyt c_{552}. It is formed of two conformationally and structurally independent domains, each one harboring one heme *c* moiety

[36]. These two domains will be referred as C-terminal (or cyt c_{550}[C]) and N-terminal (or cyt c_{550}[N]) in the following. Interestingly, the two domains exhibit different isoelectric points (5 and 7.97 for the cyt c_{550}[C] and cyt c_{550}[N] respectively), and thus opposite net charges at pH 7. It was established by stopped-flow UV/Vis experiments that the N-terminal domain only receives electrons from SOR, while both N and C-terminal are able to give them to cyt c_{552} [36]. This protein was thus proposed to function as an electron shuttle rather than an electron wire. Electrostatic forces seem to play an important role in the interaction between the N-terminal domain and both SOR and cyt c_{552}, whereas hydrophobic residues are suggested to be involved in the interaction between the C-terminal domain and cyt c_{552}.

Further insight into the function of cyt c_{550} can be obtained through the study of its redox properties. Hereafter we compare the voltammetric behavior at nanostructured gold electrodes of the full-length cyt c_{550} (23 kDa), as well as cyt c_{550}[C] (14kDa) and cyt c_{550}[N] (9 kDa), which have been separately cloned and expressed [36], and discuss it in light of related systems, such as the cyt c_4 and cyt c_{552}. To take into account the distinct surface properties of these proteins, different modifications of the gold surface were probed. The redox potentials of the hemes were also determined by potentiometric titrations followed both by UV/Vis and EPR spectroscopies, in order to identify cooperative interactions between them. Finally, coupling of electrochemistry and infrared spectroscopic techniques allowed us to monitor the conformational changes occurring in the protein and the heme cofactor during redox reaction.

2. Materials and Methods

2.1 Chemicals

Sodium citrate, hydrogen tetrachloroaurate trihydrate, mercaptopropionic acid, cysteamine, 6-mercaptohexan-1-ol, 1-hexanethiol, 6-mercaptohexanoic acid, potassium phosphate dibasic trihydrate were purchased from Sigma and were used without further purifications.

2.2 Protein samples preparation

The cyt c_{550} and its individual domains were purified based on the methods detailed previously [35, 36] with the following modifications. After protein expression due to the T7 leaky expression and periplasmic protein extraction, the extract containing full-length cyt c_{550} or cyt c_{550}[N] were dialyzed against 5 mM Tris-HCl pH 8.0 and loaded onto EMD Fractogel TMAE (Merck Millipore) and eluted with 50 mM NaCl. The pooled fractions were then concentrated in a centrifugal filter concentration (5 kDa MWCO) and diluted with 5 mM Tris-HCl pH 8.0 to reduce the salt concentration for application on a second ion exchange column of SOURCE

15Q. The bound protein was eluted 50 mM Tris-HCl and finally purified with gel filtration on Superdex 75 in 5 mM Tris-HCl buffer. For cyt c_{550}[C], the dialysis was performed against 5 mM sodium acetate pH 5.0 prior to a cation exchange chromatography on CM Sepharose. The protein was eluted with 250 mM NaCl in the acetate buffer, concentrated and applied directly on Superdex 75 gel filtration chromatography in 5 mM Tris-HCl pH 8.0, 150 mM NaCl buffer. All samples were concentrated, aliquoted and flash-frozen in liquid nitrogen prior to storage at -80 °C.

2.3 Potentiometric titrations followed by UV/Vis spectroscopy

The titrations were carried out at 12°C in an electrochemical thin layer cell closed with CaF_2 windows as described previously [37]. A mixture of 19 mediators was added to the protein sample with a final concentration of 25 µM to accelerate the redox reaction [38]. A gold grid modified with a 1:1 aqueous solution of cysteamine and mercaptopropionic acid was used as working electrode, a platinum contact as counter electrode and an aqueous Ag/AgCl 3M KCl as reference electrode. The spectra were recorded with a Cary 300 spectrometer coupled to a potentiostat. A spectrum at -0.2 V (vs Standard Hydrogen Electrode SHE) was taken as reference. Spectra were recorded every 12 mV steps for the full-length protein and 25 mV steps for the fragments. For each potential step, an average equilibration time of 10 minutes had to be applied. The potential was changed when the spectra did not evolve anymore. The differential absorbance values at 552 nm and 419 nm were plotted as a function of the applied electric potential and fitted to a Nernst equation.

2.4 Potentiometric titrations followed by EPR spectroscopy

The titrations were carried out at 15°C as described by Dutton et al. [39] in the presence of the following redox mediators at 100 µM: 2,5-dimethyl-*p*-benzoquinone, 2-hydroxy 1,2-naphthoquinone and 1,4-naphthoquinone. Reductive titrations were carried out using sodium dithionite, and oxidative titrations were carried out using ferricyanide. EPR spectra were recorded on a Bruker ElexSys X-band spectrometer fitted with an Oxford Instruments liquid-Helium cryostat and temperature control system. The same procedure of fitting as for the UV/Vis titration was applied.

2.5 Voltammetric experiments

For the cyclic voltammetry experiments, gold disk electrodes were modified by drop casting of a solution of gold nanoparticles (NPs) stabilized by citrates [27, 40]. The gold NPs of 15 nm

average diameter were prepared by the procedure of Turkevich et al. [41] and Frens [42]. The effective area of the electrode was estimated by integration of the Au-O reduction peak at 1.1 V in the cyclic voltammogram recorded in 0.1 M H_2SO_4 and taking a value of 390 $\mu C.cm^{-2}$ for a gold oxide surface [43]. Different modifications of the gold surface were probed as follows: i) 1mM solution of mercaptopropionic acid in water, ii) cysteamine in water, iii) 6-mercapto-hexanoic acid in ethanol, iv) a 1/1 mixture of 6-mercaptohexan-1-ol and 1-hexanethiol in ethanol. Then 4 µl of protein solution in pH 7 phosphate buffer were deposited on the electrode surface and left overnight at 4°C. The electrochemical measurements were performed in a standard three-electrode cell connected to a VERSASTAT 4 potentiostat (Princeton Applied Research). A 3 M NaCl AgCl/Ag was used as reference electrode and a platinum wire as counter electrode. The potentials mentioned here are referred to a standard hydrogen electrode (SHE). The cell was flushed with argon for 30 minutes prior to the measurements. Cyclic voltammograms (CVs) were recorded in 0.1 M phosphate pH 7 buffer at various scan rates between 0.1 and 3 $V.s^{-1}$. Electron transfer rates k_{ET} were determined from the anodic and cathodic peak separation, according to Laviron's theory [44, 45]. Protein coverage was estimated by integration of the cathodic and anodic peaks.

2.6 Redox-induced FTIR difference spectroscopy

Fourier transform infrared difference spectra were measured at 12°C in the same cell as the one used for UV/Vis potentiometric titrations. The cell was placed in the sample compartment of a Vertex 70 FTIR spectrometer (Bruker, Germany). Complete reduction and oxidation of the enzyme were obtained at -0.2 V and +0.5 V (vs SHE) respectively. Spectra were recorded after an equilibration time of 3 minutes for both oxidation and reduction. For each state, two spectra (256 scans and 4 cm^{-1} resolution) were recorded and averaged. The reaction was typically cycled 50-60 times and the difference spectra averaged. The spectrometer was purged with dry air, and remaining signals from humidity have been corrected.

3. Results and discussion

3.1 Potentiometric titrations followed by UV/Vis spectroscopy

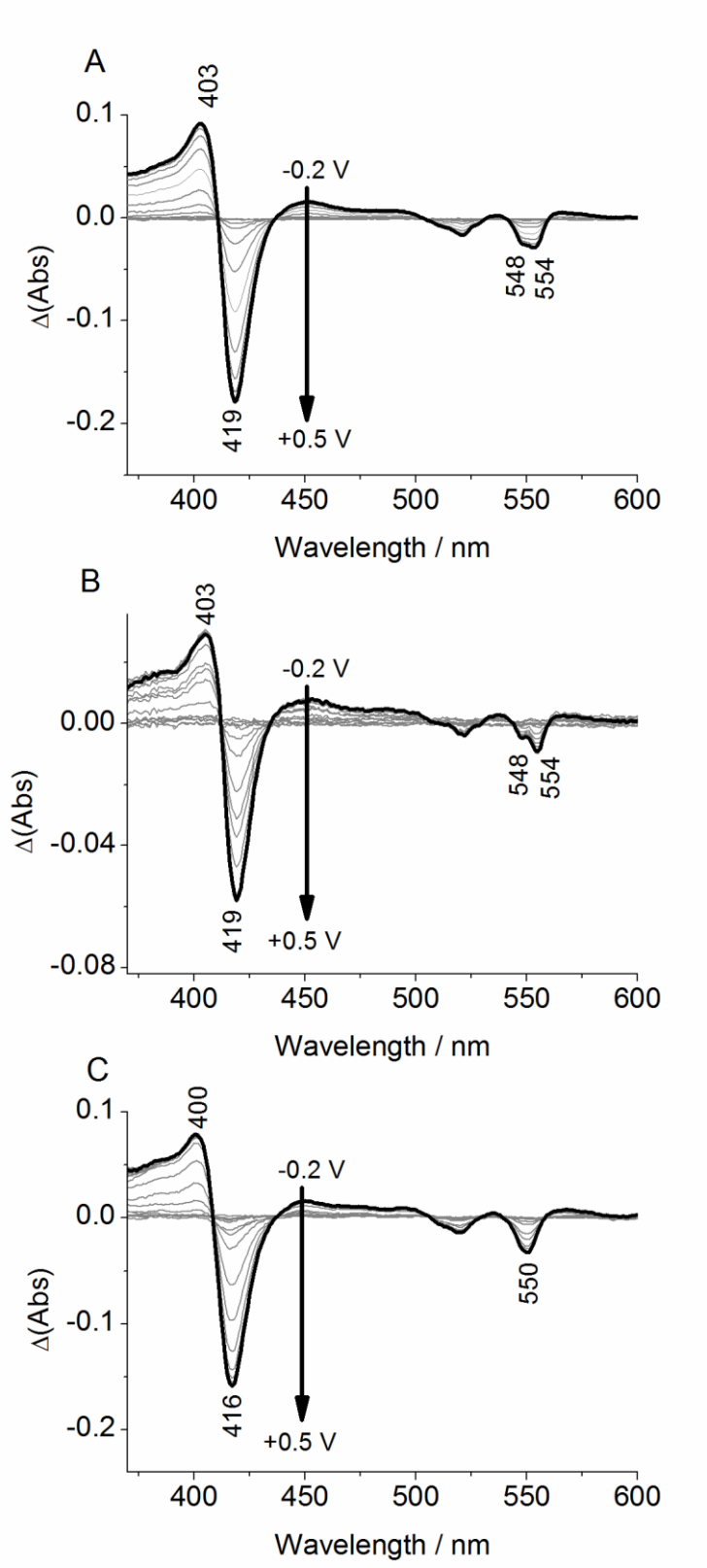

Fig. 1. Oxidized minus reduced UV Visible spectra of cyt c_{550} (A), cyt c_{550}[C] (B) and cyt c_{550}[N] (C) obtained during a redox titration from -0.2 to +0.5 V.

Fig. 1 shows the oxidized minus reduced UV/VIS difference spectra of full length cyt c_{550} (A), cyt c_{550}[C] (B) and cyt c_{550}[N] (C) obtained during a titration from -0.2 to +0.5 V. In the fully

reduced form at -0.2 V, cyt c_{550} and cyt c_{550}[C] exhibit a Soret band at 419 nm, a beta band at 520 nm and a composite alpha (α) band at 548 and 554 nm. Interestingly, for cyt c_{550}[N], the Soret band is downshifted to 416 nm, and the α-band merges to one large peak at 550 nm. In the oxidized form at +0.5 V, the Soret band is centered at 403 nm for the full-length protein and cyt c_{550}[C], and at 400 nm for cyt c_{550}[N]. These spectral shifts reveal subtle differences in the environment of the two hemes *c*.

The titration curves in the *α*-band region are shown in Fig. 2. Those in the Soret band region are available in Supporting information (Figs. S1-S3). The two cyt c_{550}[C] and cyt c_{550}[N] fragments exhibit very similar midpoint potentials values (+145 and +134 mV respectively) in spite of the structural differences of the two heme binding domains. Both can spontaneously transfer one electron to cyt c_{552}, for which a midpoint potential of +200 mV was reported [46]. The redox transitions of the full-length protein also occur in the same range of potentials, and the titration curve can be acceptably fitted with only one component at +141 mV. The similar redox potential of both hemes and the overlap of their spectral contributions in the α-band at 550 nm do not allow to distinguish them clearly in the UV/Vis potentiometric titration. In contrast, the two hemes of cyt c_4 have significantly different midpoint potentials, one above +300 mV and the second between +190 and +260 mV [31-34]. This leads to more complexity in the redox titration [32].

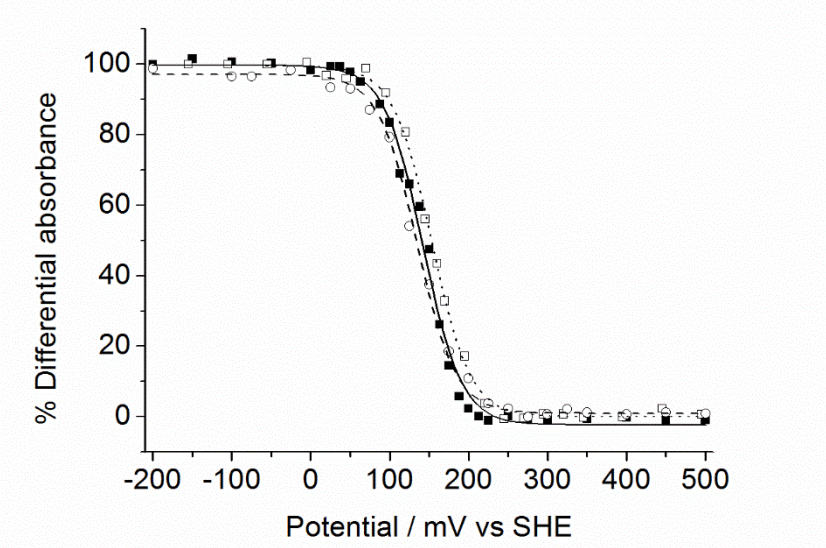

Fig. 2. UV/Vis titration curves of cyt c_{550} (black squares), cyt c_{550}[C] (open squares) and cyt c_{550}[N] (open circles) fragments. For the full-length cytochrome c_{550}, fit parameters are E_m = + 141 mV and n=1 (solid line). For the c_{550}[C] fragment, fit parameters are E_m = + 145 mV and n=1 (dotted line) and for the c_{550}[N] fragment, fit parameters are E_m = + 134 mV and n=1 (dashed line).

3.2 Potentiometric titrations followed by EPR spectroscopy

Cyt c_{550}[N] and cyt c_{550}[C] exhibit not only different optical spectra but also clear distinct EPR signatures (Fig. 3A; curves d and e). Observed g_z values are 3.138 for cyt c_{550}[N] and 2.946 for cyt c_{550}[C]. The EPR spectrum of the full-length cytochrome (Fig. 3A, curve a) shows a complex g_z signal resulting from both contributions. A careful examination of the peak reveals that it does not result from the simple addition of both isolated contributions, shown in Fig. 3A, curve b. The peak observed in the full-length protein can, however, be obtained by mixing both cyt c_{550}[N] and cyt c_{550}[C] in a single sample (curve c). This suggests that the two domains are interacting in the full-length protein, leading to a change in the cyt c_{550}[N] and cyt c_{550}[C] spectral contributions.

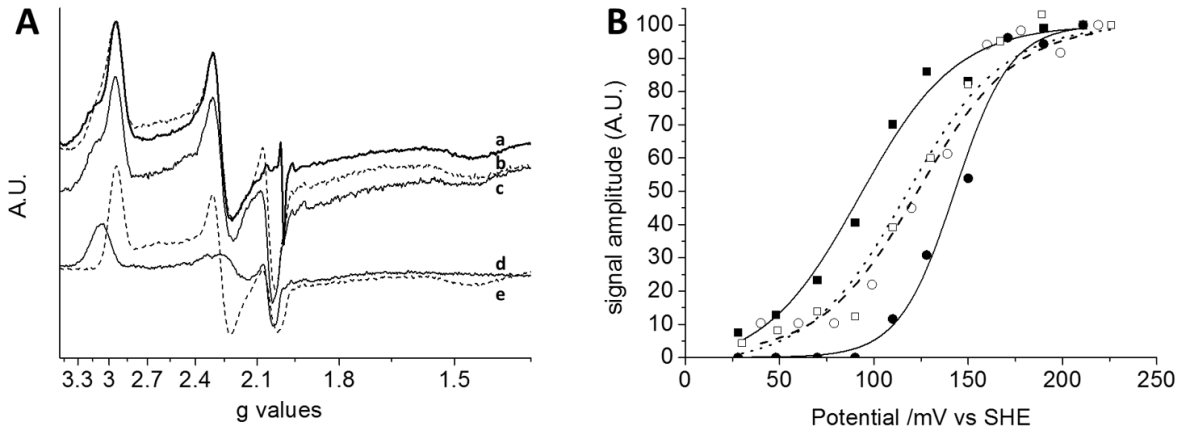

Fig. 3. (A) EPR spectra of oxidized cyt c_{550}, cyt c_{550}[N] and cyt c_{550}[C]. On the top, bold solid (a) and solid (c) lines correspond to cyt c_{550} and cyt c_{550}[N]+ cyt c_{550}[C] mixed together (1/1) respectively. The dashed line (b) corresponds to the arithmetic sum of the spectra of the fragments cyt c_{550}[N] and cyt c_{550}[C]. On the bottom, the spectra of the cyt c_{550}[N] (solid line d) and cyt c_{550}[C] (dashed line e) fragments are shown. The g_z values are 3.138 and 2.946 for the cyt c_{550}[N] and cyt c_{550}[C] fragments respectively. (B) EPR titration curves of c_{550} (closed symbols), c_{550}[N] or c_{550}[C] fragments (open symbols), at g = 3.138 (circles) and g= 2.946 (squares). For the full-length cytochrome c_{550}, fit parameters are E_m = + 92 mV and n=1 for c_{550}[C] (closed squares, solid line) and E_m = + 143 mV and n=1.8 for c_{550}[N] (closed circles, solid line). For the c_{550}[N] fragment, fit parameters are E_m = + 123 mV and n=1 (open circles, dashed line). For the c_{550}[C] fragment, fit parameters are E_m = + 121 mV and n=1 (open squares, dotted line).

The distinct cyt c_{550}[N] and cyt c_{550}[C] spectral contributions allow us to follow the titrations of each heme specifically in the full-length protein (Fig. 3B), contrary to what is possible using optical spectroscopy where the α-bands are merged to one large peak. In the full-length cyt c_{550}, fit parameters are E_m = + 92 mV and n=1 for the C-terminal and E_m = + 143 mV and n=1.8 for

the N-terminal domain. Titrations were also performed on the individual fragments (Fig. 3B). Fit parameters are E_m = + 123 mV and n=1 for cyt c_{550}[N], and E_m = + 121 mV and n=1 for cyt c_{550}[C]. Small deviations of 10-20 mV can be observed between the optical and EPR titrations of the fragments, which may be due to small shifts from the reference electrodes used in the two experiments. Nonetheless, the EPR titrations suggest that the potentiometric properties of the individual hemes are divergent in the fragments and full-length protein and they demonstrate the existence of cooperative interactions between them. This behavior was also suggested in other multi redox center proteins, including diheme cyt c_4 [33], cyt *c* oxidase [47, 48] and tetraheme cyt c_3 [49, 50]. Interestingly, as a consequence of the interaction scheme, the N-terminal domain is easier to reduce than the C-terminal domain in the full-length protein. This is consistent with the functional studies which have established that the N-terminal domain is the only one accepting electrons from the SOR and that the two domains are in rapid redox equilibrium [36]. Using the n values determined in EPR titrations, optical titrations of full-length protein can also be fitted (see Fig. S3 in Supporting information).

3.3 Cyclic voltammetry

For the voltammetric studies, the proteins were immobilized on gold nanoparticles (NPs) modified with self-assembled monolayers of different thiols. NPs allow the immobilization of a large amount of proteins and improve the electron transfer rates between the electrode and the redox active cofactors [27, 40, 51-58]. For a comparison of the signals of cyt c_{550} in presence and absence of gold nanoparticles, see Supporting information (Figs. S4-S5).

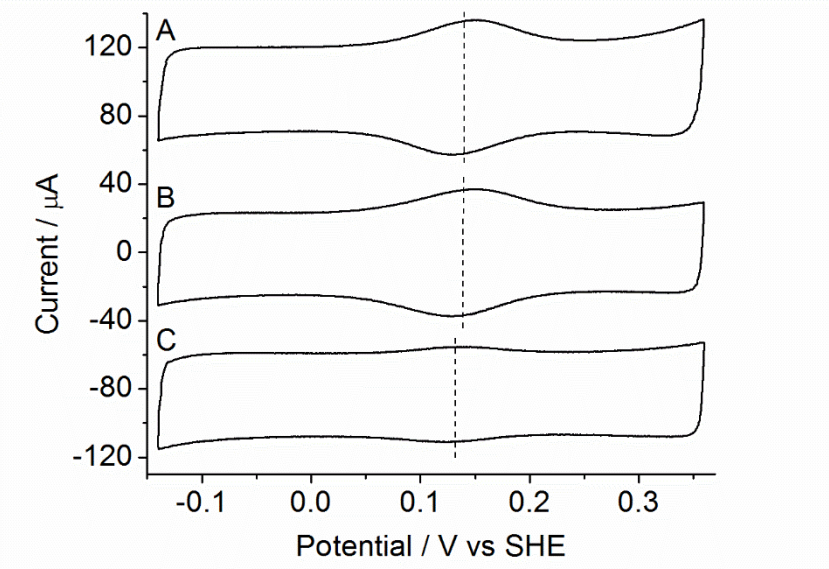

Fig. 4. Cyclic voltammograms of cyt c_{550} (A), cyt c_{550}[C] (B) and cyt c_{550}[N] (C) immobilized on gold NPs modified with mercaptopropionic acid (scan rate 0.1 V. s^{-1}, pH 7).

Negatively-charged gold surfaces at pH 7, obtained with carboxyl-terminated alkanethiols, were probed first. Fig. 4 shows the CVs of cyt c_{550}, cyt c_{550}[C] and cyt c_{550}[N] on gold NPs modified with 3-mercaptopropionic acid. A unique pair of quasi reversible anodic and cathodic signals was observed for the three protein samples. Again, this is different from cyt c_4 which exhibited four well-defined redox peaks, two in oxidation and two in reduction [31, 34]. The redox potentials, determined from the half sum of the peak potentials, are +0.14 V for both the full-length protein and the C-terminal fragment and +0.13 V for the N-terminal fragment. These values are in the same range of those determined in solution by potentiometric titrations, confirming that the interaction with the surface does not perturb the proteins structure. The protein coverage obtained by integration of the signals, the width of the peaks and the ET rate determined by Laviron's method (See Figs. S7-S14 in Supporting information) are collected in Table 1. Clearly, the surface coverage is better for cyt c_{550}[C] than for cyt c_{550}[N]. This is consistent with the net charge of the proteins, which is negative for the latter and positive for the former at pH 7, according to their isoelectric points. As expected, electrostatic forces play an important role in the interaction between these proteins and the negatively charged electrode surface. The peak width reflects the number of electrons exchanged, as well as the homogeneity of the adsorbed molecules [59, 60]. The values for the two fragments are close to the ideal value of 90 mV obtained for a rapid monoelectronic exchange to a homogenous film of adsorbates. No major difference in orientation on the surface can thus be expected for the proteins on the electrode surface. Interestingly, the peak width is also close to 90 mV for the full-length protein. The ET rates are comparable for the three samples and close to 10 s^{-1}. The size difference between these proteins can account for the small variations observed. When the chain length of the thiol was increased from 3 to 6 carbons, the anodic and cathodic peak separation increased for the three samples (see Fig. S6 in Supporting information), and a moderate decrease of the ET rate was determined. With mercaptoundecanoic acid, in contrast, the anodic and cathodic signals were no longer observed, suggesting a larger decrease in the ET. These results are consistent with previous studies on mitochondrial cyt *c* [7, 9, 17] as well as other small soluble proteins [61, 62], which showed an almost distance-independent measured rate for short-length thiols (C_1-C_{10}) and an exponential decrease of the ET rate for longer ones. We also note that the width of the peaks is larger for the proteins immobilized on mercaptohexanoic acid than on mercaptopropionic acid.

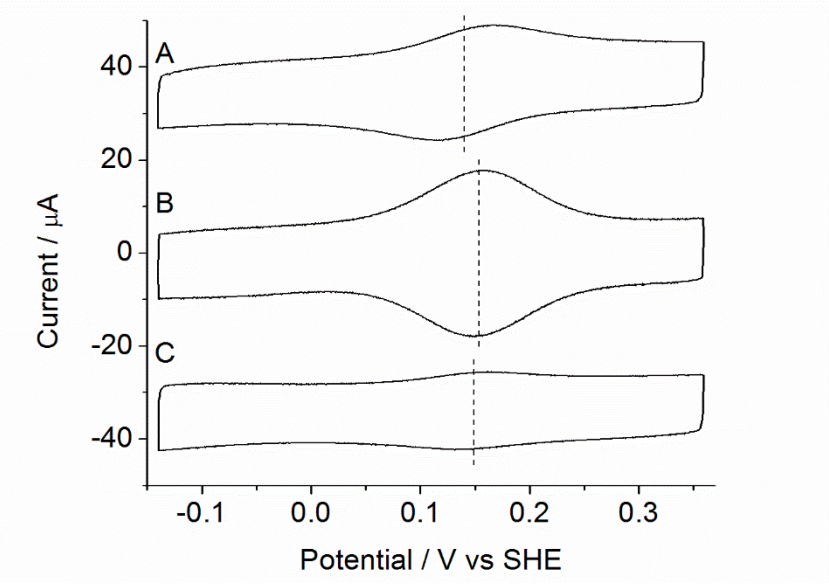

Fig. 5. Cyclic voltammograms of cyt c_{550} (A), cyt c_{550}[C] (B) and cyt c_{550}[N] (C) immobilized on gold NPs modified with a 1/1 mixture of 6-mercaptohexan-1-ol and 1-hexanethiol (scan rate 0.1 $V.s^{-1}$, pH 7).

Well-defined anodic and cathodic signals at similar potential values were also obtained on gold NPs surfaces modified with a 1/1 mixture of 6-mercaptohexan-1-ol and 1-hexanethiol (see Fig. 5). This neutral and hydrophobic blend of modifiers was chosen because it was well adapted to the immobilization of cyt c_{552} [27], one of the electron partner of cyt c_{550}. In addition, cyt c_{552} exhibits a high sequence similarity with cyt c_{550}[C]. Both proteins share in particular a hydrophobic belt around the heme cleft [36]. Interestingly, despite its net positive charge at pH 7, cyt c_{550}[C] exhibited a similar coverage and a twice as high electron exchange rate on these neutral surfaces than on the previously studied negatively charged ones (see Table 1). This observation may be of functional significance for the recognition between cyt c_{550}[C] and cyt c_{552}, which is believed to involve apolar interactions. For cyt c_{550}[N] and the full length *cyt* c_{550} protein electron transfer was also faster on gold NPs modified with 6-mercaptohexan-1-ol and 1-hexanethiol than on those modified with ω-carboxyl alkanethiols. It is likely that the absence of charge repulsion allows the protein to be closer to the surface. The width of the peaks is larger than 90 mV in all cases, which suggests that a larger distribution of microenvironments is available for the adsorbed proteins. This was also observed for cyt c_{552} before [27].

On positively-charged gold surfaces modified with cysteamine, in contrast, only broad and weak signals were observed for the three protein samples at both, high and low ionic strength. This was unexpected for cyt c_{550}[N], which bears a negative charge at pH 7. This suggests that no specific orientation of the protein for efficient electron transfers occurs on these surfaces,

and that ionic interactions may not be the only one involved in the interaction between cyt c_{550}[N] and the SOR.

Table 1. protein coverage (Γ), electron transfer rate (k_{ET}), redox potential (E°) and full width at half height of the anodic peak (Fwhh) of cyt c_{550}, cyt c_{550}[C] and cyt c_{550}[C] immobilized on gold NPs modified with either mercaptopropionic acid (MPA), or mercaptohexanoic acid (MHA), or a 1/1 mixture of 6-mercaptohexan-1-ol and 1-hexanethiol in ethanol (MIXT).

Protein/ Surface modification	**Γ/pmol.cm^{-2}**	**k_{ET}/s^{-1}**	**E°/mV**	**Fwhh/mV**
Cyt c_{550}/MPA	2	9	140	90
Cyt c_{550}[C]/MPA	5	11	141	91
Cyt c_{550}[N]/MPA	1	14	132	84
Cyt $_{550}$/MHA	1	2	141	106
Cyt c_{550}[C]/MHA	1	0.8	140	107
Cyt c_{550}[N]/MHA	2	4	130	123
Cyt c_{550}/MIXT	1	19	142	115
Cyt c_{550}[C]/MIXT	5	24	154	114
Cyt c_{550}[N]/MIXT	1	29	149	100

3.4 FTIR difference spectroscopy

Redox-driven changes in the environment of the cofactors, polypeptide backbone and protonation of key amino acid residues occurring upon electron transfer were monitored by infrared difference spectroscopy. The oxidized-minus-reduced difference spectra obtained for cyt c_{550}[C] and cyt c_{550}[N] for a potential step from -0.2 to +0.5 V (vs. SHE) at pH 7 are shown in Fig. 6. For comparison purposes, the spectrum of *T. thermophilus* cyt c_{552} [63] is also shown. In these spectra, the positive signals correspond to the oxidized state of the protein and the negative signals to the reduced state.

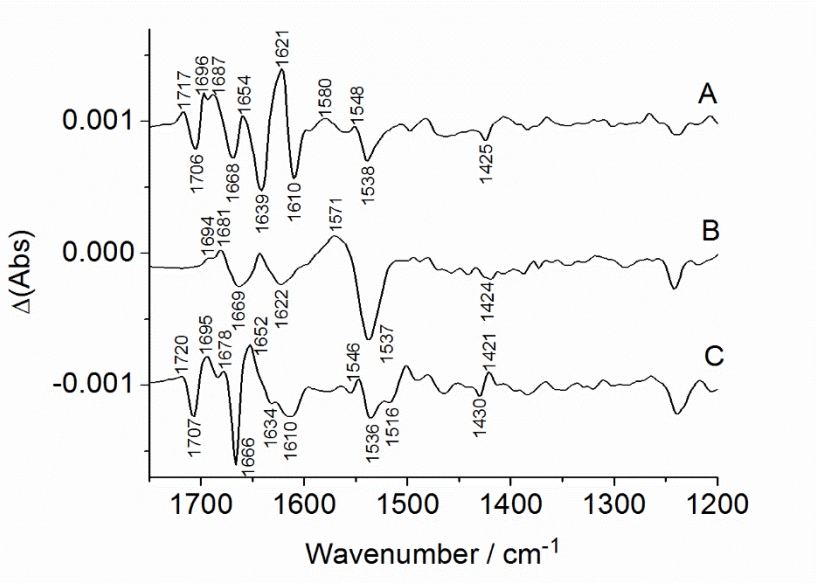

Fig 6. Oxidized minus reduced Fourier transform infrared spectra of cyt c_{550}[C] (A), cyt c_{550}[N] (B) and cyt c_{552} (C).

The difference spectra of cyt c_{550}[C] and cyt c_{552} exhibit some similarities. This was expected, when considering the high sequence homology of the two proteins. Several signals arise from the protein backbone. The so-called amide I mode includes the ν(C=O) vibrational mode and is observed between 1700 and 1600 cm^{-1}. The bands in this region correspond to different secondary structure elements of the protein [64-66]. For cyt c_{552}, the most intense signal is seen at 1666 cm^{-1} and corresponds to the rearrangement of β-turns, whereas for cyt c_{550}[C] it is the signal of β-sheets at 1641 cm^{-1} which dominates in this region. In the amide II range (1570-1530 cm^{-1}) the signals from coupled CN stretching and NH deformations are expected. These modes probably contribute at 1548/1538 and 1546/1536 cm^{-1} for cyt c_{550}[C] and cyt c_{552} respectively. The bands at 1707 (-), 1695 (+), 1687 (+) and 1678 (+) cm^{-1} can be assigned to ν(C=O) modes of protonated heme propionates [67, 68]. These relatively high wavenumbers confirm that the hemes are surrounded by a rather hydrophobic environment. The positive signal observed at 1717 cm^{-1} and 1720 cm^{-1} for cyt c_{550}[C] and cyt c_{552} can be attributed to an Asp or Glu residue [38, 66, 69-71] which is protonated in the oxidized form and probably located in the hydrophobic environment surrounding the heme. Deprotonated propionates and acidic residues contribute between 1580 and 1520 cm^{-1} ($\nu(COO^-)^{as}$ mode) and between 1480 and 1320 cm^{-1} ($\nu(COO^-)^{s}$ mode) [38].

The spectrum of cyt c_{550}[N] shows no similarity with those of cyt c_{550}[C] and cyt c_{552}, which confirms that the two domains are structurally distinct. Contributions in the amide I region are broad and can be assigned mainly to the rearrangements of β-turns (1669 cm^{-1}). Signals of the protonated heme propionates can be seen for the oxidized state at 1694 and 1681 cm^{-1}. In

contrast with cyt c_{550}[C], no signal from Asp or Glu residue above 1700 cm^{-1} is evident in the spectrum.

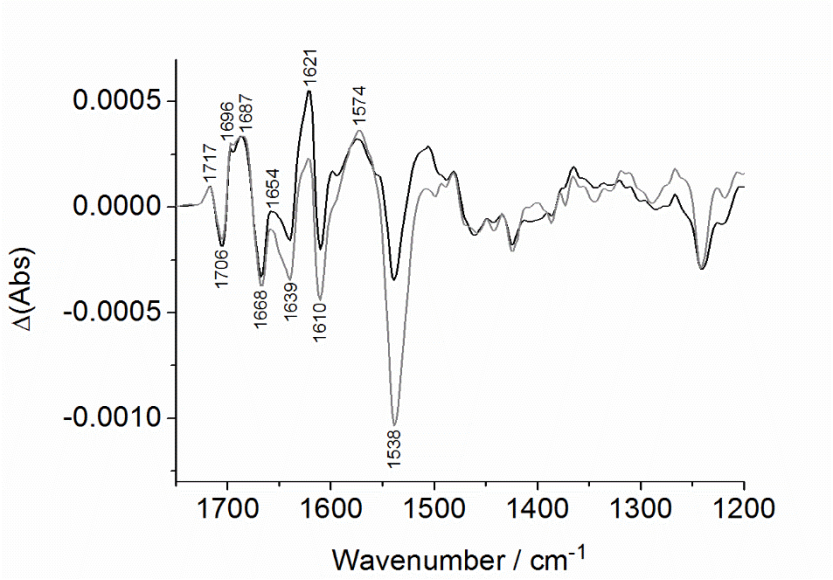

Fig 7. Comparison between the oxidized minus reduced Fourier transform infrared spectra of cyt c_{550} (black plot), and the arithmetic sum of the spectra cyt c_{550}[C] and cyt c_{550}[N] (grey plot).

Fig. 7 shows the difference spectrum of the full-length protein. Clearly, the C-terminal domain contributes the most to the spectrum and the characteristic signals of β-turn at 1666 cm^{-1}, β-sheets at 1639 cm^{-1}, heme propionates at 1706, 1696 and 1687 cm^{-1} and protonated Asp or Glu at 1720 cm^{-1} described before for cyt c_{550}[C] can also be seen for cyt c_{550}. In order to determine how both domains are perturbed by the linkage between both, the arithmetic sum of the spectra of the two fragments is shown in Fig. 7, in direct comparison with the spectrum of the full-length protein. Major differences between the two spectra can be seen in the amide I range (β-turn and β-sheets signals) and in the amide II range (1570-1530 cm^{-1}). This is probably due to a lower conformational flexibility for the full-length protein than for the fragments. Interestingly, the signals of the heme propionates and protonated Asp or Glu are barely affected.

4. Conclusion

Both voltammetric studies and potentiometric titrations show that the hemes of the cyt c_{550}[C] and cyt c_{550}[N] fragments have very close mid potentials values. In the full-length protein, however, EPR studies suggest that the N-terminal heme is easier to reduce than the C-terminal due to cooperative interactions. Interestingly, efficient electron transfer rates were observed on gold surfaces modified either with negatively-charged ω-carboxyl alkanethiols or a

hydrophobic mixture of 6-mercaptohexan-1-ol and 1-hexanethiol. This confirms the high versatility of this diheme protein which is able to interact with its SOR and cyt c_{552} partners either through electrostatic or hydrophobic interactions. The redox induced FTIR spectra clearly show that the C and N-terminal domains are structurally very different and that the C-terminal domain is structurally related to cyt c_{552}.

Acknowledgements

FM and PH are grateful to the icFRC Labex, the CNRS and the University of Strasbourg for financial support. SA is a PhD student supported by a grant from the Libyan Ministry of Education. Part of this study was also facilitated by a HEA grant under the Programme for Research in Third-Level Institutions (PRTLI 5) of the University of Limerick. BSC is grateful to the EPR facilities available at the Aix-Marseille University EPR center, and to financial support from the French EPR network (RENARD, IR3443).

References

[1] J.N. Onuchic, D.N. Beratan, J.R. Winkler, H.B. Gray, Pathway analysis of protein electron-transfer reactions, Annu. Rev. Biophys. Biomol. Struct., 21 (1992) 349-377.
[2] C.C. Page, C.C. Moser, X. Chen, P.L. Dutton, Natural engineering principles of electron tunnelling in biological oxidation-reduction, Nature, 402 (1999) 47-52.
[3] C.C. Page, C.C. Moser, P.L. Dutton, Mechanism for electron transfer within and between proteins, Curr. Opin. Chem. Biol., 7 (2003) 551-556.
[4] S. Rackovsky, D.A. Goldstein, On the redox conformational change in cytochrome c, Proc. Natl. Acad. Sci. USA, 81 (1984) 5901-5905.
[5] T. Takano, R.E. Dickerson, Conformation change of cytochrome c, J. Mol. Biol., 153 (1981) 95-115.
[6] G.W. Bushnell, G.V. Louie, G.D. Brayer, High-resolution three-dimensional structure of horse heart cytochrome c, J. Mol. Biol., 214 (1990) 585-595.
[7] L. Rivas, D.H. Murgida, P. Hildebrandt, Conformational and Redox Equilibria and Dynamics of Cytochrome c Immobilized on Electrodes via Hydrophobic Interactions, J. Phys. Chem. B, 106 (2002) 4823-4830.
[8] M.J. Eddowes, H.A.O. Hill, Electrochemistry of horse heart cytochrome c, J. Am. Chem. Soc., 101 (1979) 4461-4464.
[9] J. Wei, H. Liu, D.E. Khoshtariya, H. Yamamoto, A. Dick, D.H. Waldeck, Electron-Transfer Dynamics of Cytochrome C: A Change in the Reaction Mechanism with Distance, Angew. Chem. Int. Ed., 41 (2002) 4700-4703.
[10] X. Chen, R. Ferrigno, J. Yang, G.M. Whitesides, Redox Properties of Cytochrome c Adsorbed on Self-Assembled Monolayers: A Probe for Protein Conformation and Orientation, Langmuir, 18 (2002) 7009-7015.
[11] G.-X. Wang, M. Wang, Z.-Q. Wu, W.-J. Bao, Y. Zhou, X.-H. Xia, Dependence of the direct electron transfer activity and adsorption kinetics of cytochrome c on interfacial charge properties, Analyst, 138 (2013) 5777-5782.
[12] M.J. Tarlov, E.F. Bowden, Electron-transfer reaction of cytochrome c adsorbed on carboxylic acid terminated alkanethiol monolayer electrodes, J. Am. Chem. Soc., 113 (1991) 1847-1849.
[13] M.C. Leopold, E.F. Bowden, Influence of Gold Substrate Topography on the Voltammetry of Cytochrome c Adsorbed on Carboxylic Acid Terminated Self-Assembled Monolayers, Langmuir, 18 (2002) 2239-2245.

[14] R.A. Clark, E.F. Bowden, Voltammetric Peak Broadening for Cytochrome c/Alkanethiolate Monolayer Structures: Dispersion of Formal Potentials, Langmuir, 13 (1997) 559-565.
[15] Y.-C. Liu, S.-Q. Cui, J. Zhao, Z.-S. Yang, Direct electrochemistry behavior of cytochrome c/l-cysteine modified electrode and its electrocatalytic oxidation to nitric oxide, Bioelectrochemistry, 70 (2007) 416-420.
[16] S. Terrettaz, J. Cheng, C.J. Miller, R.D. Guiles, Kinetic Parameters for Cytochrome c via Insulated Electrode Voltammetry, J. Am. Chem. Soc., 118 (1996) 7857-7858.
[17] D.H. Murgida, P. Hildebrandt, Proton-Coupled Electron Transfer of Cytochrome c, J. Am. Chem. Soc., 123 (2001) 4062-4068.
[18] H. Yue, D.H. Waldeck, Understanding interfacial electron transfer to monolayer protein assemblies, Curr. Opin. Solid State Mater. Sci., 9 (2005) 28-36.
[19] H. Yue, D.H. Waldeck, J. Petrović, R.A. Clark, The Effect of Ionic Strength on the Electron-Transfer Rate of Surface Immobilized Cytochrome c, J. Phys. Chem. B, 110 (2006) 5062-5072.
[20] D.H. Murgida, P. Hildebrandt, Disentangling interfacial redox processes of proteins by SERR spectroscopy, Chem. Soc. Rev., 37 (2008) 937-945.
[21] M. Sezer, D. Millo, I.M. Weidinger, I. Zebger, P. Hildebrandt, Analyzing the catalytic processes of immobilized redox enzymes by vibrational spectroscopies, IUBMB Life, 64 (2012) 455-464.
[22] R.A. Capaldi, V. Darley-Usmar, S. Fuller, F. Millett, Structural and functional features of the interaction of cytochrome c with complex III and cytochrome c oxidase, FEBS Lett., 138 (1982) 1-7.
[23] F. Millett, C. De Jong, L. Paulson, R.A. Capaldi, Identification of specific carboxylate groups on cytochrome c oxidase that are involved in binding cytochrome c, Biochemistry, 22 (1983) 546-552.
[24] W.H. Koppenol, E. Margoliash, The asymmetric distribution of charges on the surface of horse cytochrome c. Functional implications, J. Biol. Chem., 257 (1982) 4426-4437.
[25] M.E. Than, P. Hof, R. Huber, G.P. Bourenkov, H.D. Bartunik, G. Buse, T. Soulimane, Thermus thermophilus cytochrome-c552: a new highly thermostable cytochrome-c structure obtained by MAD phasing1, J. Mol. Biol., 271 (1997) 629-644.
[26] S. Bernad, T. Soulimane, S. Lecomte, Redox and conformational equilibria of cytochrome c552 from Thermus thermophilus adsorbed on a chemically modified silver electrode probed by surface-enhanced resonance Raman spectroscopy, J. Raman Spectrosc., 35 (2004) 47-54.
[27] T. Meyer, J. Gross, C. Blanck, M. Schmutz, B. Ludwig, P. Hellwig, F. Melin, Electrochemistry of Cytochrome c1, Cytochrome c552, and CuA from the Respiratory Chain of Thermus thermophilus Immobilized on Gold Nanoparticles, J. Phys. Chem. B, 115 (2011) 7165-7170.
[28] A. Giuffrè, E. Forte, G. Antonini, E. D'Itri, M. Brunori, T. Soulimane, G. Buse, Kinetic Properties of ba3 Oxidase from Thermus thermophilus: Effect of Temperature, Biochemistry, 38 (1999) 1057-1065.
[29] J.A. Lyons, D. Aragao, O. Slattery, A.V. Pisliakov, T. Soulimane, M. Caffrey, Structural insights into electron transfer in caa3-type cytochrome oxidase, Nature, 487 (2012) 514-518.
[30] G. Moore, G.W. Pettigrew, Cytochromes c. Evolutionary, Structural and Physicochemical Aspects, Springer-Verlag, Berlin-Heidelberg-New York, 1990.
[31] H.-Y. Chang, Y. Ahn, L.A. Pace, M.T. Lin, Y.-H. Lin, R.B. Gennis, The Diheme Cytochrome c4 from Vibrio cholerae Is a Natural Electron Donor to the Respiratory cbb3 Oxygen Reductase, Biochemistry, 49 (2010) 7494-7503.
[32] F.A. Leitch, K.R. Brown, G.W. Pettigrew, Complexity in the redox titration of the dihaem cytochrome c4, Biochim. Biophys. Acta, 808 (1985) 213-218.
[33] L.S. Conrad, J.J. Karlsson, J. Ulstrup, Electron Transfer and Spectral α-Band Properties of the Di-Heme Protein Cytochrome c4 from Pseudomonas Stutzeri, Eur. J. Biochem., 231 (1995) 133-141.
[34] J.-J. Karlsson, M.F. Nielsen, M.H. Thuesen, J. Ulstrup, Electrochemistry of Cytochrome c4 from Pseudomonas stutzeri, J. Phys. Chem. B, 101 (1997) 2430-2436.
[35] S. Robin, M. Arese, E. Forte, P. Sarti, A. Giuffrè, T. Soulimane, A Sulfite Respiration Pathway from Thermus thermophilus and the Key Role of Newly Identified Cytochrome c550, J Bacteriol, 193 (2011) 3988-3997.
[36] S. Robin, M. Arese, E. Forte, P. Sarti, O. Kolaj-Robin, A. Giuffrè, T. Soulimane, Functional Dissection of the Multi-Domain Di-Heme Cytochrome c550 from Thermus thermophilus, PLOS ONE, 8 (2013) e55129.

[37] D. Moss, E. Nabedryk, J. Breton, W. Mäntele, Redox-linked conformational changes in proteins detected by a combination of infrared spectroscopy and protein electrochemistry, Eur. J. Biochem., 187 (1990) 565-572.
[38] P. Hellwig, J. Behr, C. Ostermeier, O.-M.H. Richter, U. Pfitzner, A. Odenwald, B. Ludwig, H. Michel, W. Mäntele, Involvement of Glutamic Acid 278 in the Redox Reaction of the Cytochrome c Oxidase from Paracoccus denitrificans Investigated by FTIR Spectroscopy, Biochemistry, 37 (1998) 7390-7399.
[39] P.L. Dutton, J.S. Leigh, Electron spin resonance characterization of Chromatium D hemes, non-heme irons and the components involved in primary photochemistry, Biochim. Biophys. Acta, 314 (1973) 178-190.
[40] T. Meyer, F. Melin, H. Xie, I. von der Hocht, S.K. Choi, M.R. Noor, H. Michel, R.B. Gennis, T. Soulimane, P. Hellwig, Evidence for Distinct Electron Transfer Processes in Terminal Oxidases from Different Origin by Means of Protein Film Voltammetry, J. Am. Chem. Soc., 136 (2014) 10854-10857.
[41] J. Turkevich, P.C. Stevenson, J. Hillier, A study of the nucleation and growth processes in the synthesis of colloidal gold, Discuss. Faraday. Soc., 11 (1951) 55-75.
[42] G. Frens, Controlled nucleation for the regulation of the particle size in monodisperse gold suspensions, Nat. Phys. Sci., 241 (1973) 20-22.
[43] S. Trasatti, O.A. Petrii, Real surface area measurements in electrochemistry, J. Electroanal. Chem., 327 (1992) 353-376.
[44] E. Laviron, General expression of the linear potential sweep voltammogram in the case of diffusionless electrochemical systems, J. Electroanal. Chem., 101 (1979) 19-28.
[45] R. Campos, E.E. Ferapontova, Electrochemistry of weakly adsorbed species: Voltammetric analysis of electron transfer between gold electrodes and Ru hexaamine electrostatically interacting with DNA duplexes, Electrochim. Acta, 126 (2014) 151-157.
[46] J.A. Fee, Y. Chen, T.R. Todaro, K.L. Bren, K.M. Patel, M.G. Hill, E. Gomez-Moran, T.M. Loehr, J. Ai, L. Thöny-meyer, P.A. Williams, E. Sturam, V. Sridhar, D.E. McRee, Integrity of thermus thermophilus cytochrome c552 Synthesized by escherichia coli cells expressing the host-specific cytochrome c maturation genes, ccmABCDEFGH: Biochemical, spectral, and structural characterization of the recombinant protein, Protein Sci., 9 (2000) 2074-2084.
[47] D.F. Wilson, J.G. Lindsay, E.S. Brocklehurst, Heme-heme interaction in cytochrome oxidase, Biochim. Biophys. Acta, 256 (1972) 277-286.
[48] P. Nicholls, L.C. Petersen, Haem—haem interactions in cytochrome aa3 during the anaerobic-aerobic transition, Biochim. Biophys. Acta, 357 (1974) 462-467.
[49] H. Santos, J.J.G. Moura, I. Moura, J. LeGall, A.V. Xavier, NMR studies of electron transfer mechanisms in a protein with interacting redox centres: Desulfovibrio gigas cytochrome c3, Eur. J. Biochem., 141 (1984) 283-296.
[50] M. Coletta, T. Catarino, J. LeGall, A.V. Xavier, A thermodynamic model for the cooperative functional properties of the tetraheme cytochrome c3 from Desulfovibrio gigas, Eur. J. Biochem., 202 (1991) 1101-1106.
[51] Y. Xiao, F. Patolsky, E. Katz, J.F. Hainfeld, I. Willner, "Plugging into Enzymes": Nanowiring of Redox Enzymes by a Gold Nanoparticle, Science, 299 (2003) 1877-1881.
[52] J.-J. Feng, G. Zhao, J.-J. Xu, H.-Y. Chen, Direct electrochemistry and electrocatalysis of heme proteins immobilized on gold nanoparticles stabilized by chitosan, Anal. Biochem., 342 (2005) 280-286.
[53] P.S. Jensen, Q. Chi, F.B. Grumsen, J.M. Abad, A. Horsewell, D.J. Schiffrin, J. Ulstrup, Gold Nanoparticle Assisted Assembly of a Heme Protein for Enhancement of Long-Range Interfacial Electron Transfer, J. Phys. Chem. C, 111 (2007) 6124-6132.
[54] M.A. Rahman, H.-B. Noh, Y.-B. Shim, Direct Electrochemistry of Laccase Immobilized on Au Nanoparticles Encapsulated-Dendrimer Bonded Conducting Polymer: Application for a Catechin Sensor, Anal. Chem., 80 (2008) 8020-8027.
[55] J.M. Abad, M. Gass, A. Bleloch, D.J. Schiffrin, Direct Electron Transfer to a Metalloenzyme Redox Center Coordinated to a Monolayer-Protected Cluster, J. Am. Chem. Soc., 131 (2009) 10229-10236.
[56] K. Monsalve, M. Roger, C. Gutierrez-Sanchez, M. Ilbert, S. Nitsche, D. Byrne-Kodjabachian, V. Marchi, E. Lojou, Hydrogen bioelectrooxidation on gold nanoparticle-based electrodes modified by Aquifex aeolicus hydrogenase: Application to hydrogen/oxygen enzymatic biofuel cells, Bioelectrochemistry, 106, Part A (2015) 47-55.

[57] D. Fapyane, E.E. Ferapontova, Enhanced electron transfer between gold nanoparticles and horseradish peroxidase reconstituted onto alkanethiol-modified hemin, Electrochem. Commun., 70 (2016) 39-42.
[58] F. Melin, H. Xie, T. Meyer, Y.O. Ahn, R.B. Gennis, H. Michel, P. Hellwig, The unusual redox properties of C-type oxidases, Biochim. Biophys. Acta, 1857 (2016) 1892-1899.
[59] A.J. Bard, L.L. Faulkner, Electrochemical Methods, Fundamentals and Applications, John Wiley & Sons, 2001.
[60] J.N. Butt, F.A. Armstrong, Voltammetry of Adsorbed Redox Enzymes: Mechanisms in The Potential Dimension, in: O. Hammerich, J. Ulstrup (Eds.) Bioinorganic Electrochemistry, Springer Netherlands, Dordrecht, 2008, pp. 91-128.
[61] Q. Chi, J. Zhang, J.E.T. Andersen, J. Ulstrup, Ordered Assembly and Controlled Electron Transfer of the Blue Copper Protein Azurin at Gold (111) Single-Crystal Substrates, J. Phys. Chem. B, 105 (2001) 4669-4679.
[62] K. Fujita, N. Nakamura, H. Ohno, B.S. Leigh, K. Niki, H.B. Gray, J.H. Richards, Mimicking Protein−Protein Electron Transfer: Voltammetry of Pseudomonas aeruginosa Azurin and the Thermus thermophilus CuA Domain at ω-Derivatized Self-Assembled-Monolayer Gold Electrodes, J. Am. Chem. Soc., 126 (2004) 13954-13961.
[63] Y. Neehaul, Y. Chen, C. Werner, J.A. Fee, B. Ludwig, P. Hellwig, Electrochemical and infrared spectroscopic analysis of the interaction of the CuA domain and cytochrome c552 from Thermus thermophilus, Biochim. Biophys. Acta, 1817 (2012) 1950-1954.
[64] A. Dong, P. Huang, W.S. Caughey, Protein secondary structures in water from second-derivative amide I infrared spectra, Biochemistry, 29 (1990) 3303-3308.
[65] A. Dong, P. Huang, W.S. Caughey, Redox-dependent changes in beta.-extended chain and turn structures of cytochrome c in water solution determined by second derivative amide I infrared spectra, Biochemistry, 31 (1992) 182-189.
[66] A. Barth, Infrared spectroscopy of proteins, Biochim. Biophys. Acta, 1767 (2007) 1073-1101.
[67] J. Behr, P. Hellwig, W. Mäntele, H. Michel, Redox Dependent Changes at the Heme Propionates in Cytochrome c Oxidase from Paracoccus denitrificans: Direct Evidence from FTIR Difference Spectroscopy in Combination with Heme Propionate 13C Labeling, Biochemistry, 37 (1998) 7400-7406.
[68] J. Behr, H. Michel, W. Mäntele, P. Hellwig, Functional Properties of the Heme Propionates in Cytochrome c Oxidase from Paracoccus denitrificans. Evidence from FTIR Difference Spectroscopy and Site-Directed Mutagenesis, Biochemistry, 39 (2000) 1356-1363.
[69] M. Wolpert, P. Hellwig, Infrared spectra and molar absorption coefficients of the 20 alpha amino acids in aqueous solutions in the spectral range from 1800 to 500 cm−1, Spectrochim. Acta A, 64 (2006) 987-1001.
[70] F. Siebert, W. Mäntele, W. Kreutz, Evidence for the protonation of two internal carboxylic groups during the photocycle of bacteriorhodopsin, FEBS Lett., 141 (1982) 82-87.
[71] J. Zhang, W. Oettmeier, R.B. Gennis, P. Hellwig, FTIR Spectroscopic Evidence for the Involvement of an Acidic Residue in Quinone Binding in Cytochrome bd from Escherichia coli, Biochemistry, 41 (2002) 4612-4617.

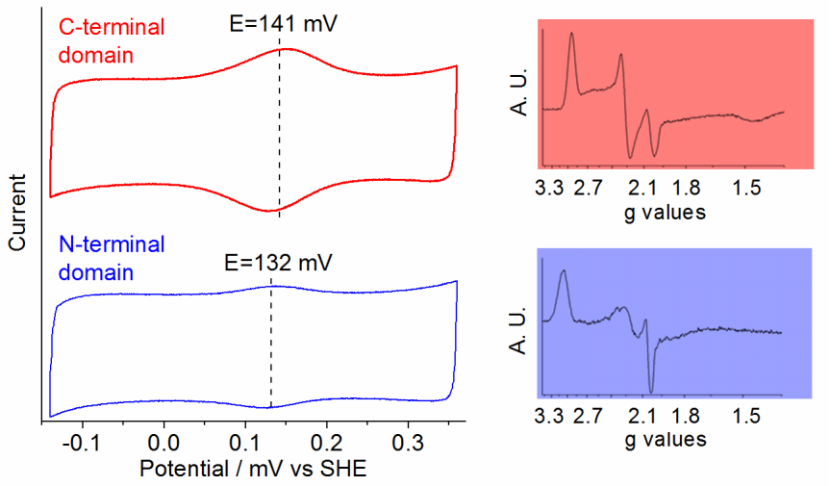

Graphical abstract